ELSEVIER

Ceramics International 33 (2007) 1083–1086

CERAMICS INTERNATIONAL

www.elsevier.com/locate/ceramint

Processing and dielectric properties of (Pb,Bi)(Mg,Nb,Ti)O_3 ceramics

Yoon-Sung Kim [a], Nam-Kyoung Kim [a,*], Jaejung Ko [b]

[a] *Department of Inorganic Materials Engineering, Kyungpook National University, Daegu 702-701, Republic of Korea*
[b] *Department of Chemistry, Korea University, Chochiwon, Chungnam 339-700, Republic of Korea*

Received 22 December 2005; received in revised form 10 February 2006; accepted 22 March 2006
Available online 10 July 2006

Abstract

Powders of the $Pb(Mg_{1/3}Nb_{2/3})O_3$–$Bi(Mg_{2/3}Nb_{1/3})O_3$ (PMN–BMN) system with $PbTiO_3$ (PT) substitution levels of 20 and 30 mol% were prepared by a B-site precursor method. Phase development as well as dielectric properties were examined. Two major phases, i.e., $MgNb_2O_6$ and $[(Mg_{1/3}Nb_{2/3})_{1/2}Ti_{1/2}]O_2$ (with small fractions of $Mg_4Nb_2O_9$), developed in the B-site precursor compositions, whereas only monophasic perovskite formed after the addition of PbO/Bi_2O_3. Maximum dielectric constant values of the two systems decreased rapidly with increasing BMN concentration, but corresponding temperatures were lowest at intermediate compositions.

Keywords: A. Powders: solid-state reaction; B. X-ray methods; C. Dielectric properties; Ceramics; Perovskite oxides

1. Introduction

Lead magnesium niobate $Pb(Mg_{1/3}Nb_{2/3})O_3$ is a widely investigated relaxor of a complex-perovskite structure. Characteristic features of PMN include very high maximum dielectric constants (as high as 20,000 at slightly below room temperature) with diffuse phase transition [1–3]. Lead titanate $PbTiO_3$ is also a perovskite compound, but with sharp phase transition modes and very high Curie temperature of 490 °C. The two compounds had been synthesized readily to a perovskite structure by the columbite process [4,5] and one-step solid-state reactions, respectively.

To the authors' knowledge, however, perovskite bismuth magnesium niobate $Bi(Mg_{2/3}Nb_{1/3})O_3$ has not been synthesized so far, even though the electron configurations of Bi^{3+} and Pb^{2+} are identical: $[Xe]4f^{14}5d^{10}6s^2$. In addition, $Bi(Mg_{2/3}Nb_{1/3})O_3$ is similar to $Pb(Mg_{1/3}Nb_{2/3})O_3$ in stoichiometry, except for the alteration in the Mg:Nb ratio of 1:2 (in PMN) to 2:1 to compensate for the charge difference between Pb^{2+} and Bi^{3+}. The inability of perovskite formation in BMN may be attributed to the somewhat small size of Bi [6] to fit in the 12-fold cubo-octahedral sites of the perovskite structure. The failure may also be attributed to the comparatively strong covalent coupling of Bi–O [7], which may arise from a smaller electronegativity difference than the Pb-compound.

Preparation of PMN–BMN [8] as well as the system with 10 mol% PT substitution [9] has been attempted, where the maximum dielectric constant values decreased sharply with increasing BMN concentration. In the present study, therefore, the substitution level of PT was further increased to 20 and 30 mol%. Changes in the dielectric properties were investigated and the results are compared with the previous data. In order to promote the perovskite formation in the present BMN-containing compositions, ceramic powders were prepared by a B-site precursor method [10,11], which is conceptually identical to the columbite process.

2. Experimental

The two investigated systems of PMN–BMN, with 20 and 30 mol% PT substitution, are $(0.8-x)$PMN–xBMN–0.2PT and $(0.7-y)$PMN–yBMN–0.3PT, i.e., $(Pb_{1-x}Bi_x)(Mg_{(0.8+x)/3}Nb_{(1.6-x)/3}Ti_{0.2})O_3$ and $(Pb_{1-y}Bi_y)(Mg_{(0.7+y)/3}Nb_{(1.4-y)/3}Ti_{0.3})O_3$ (Systems I and II), respectively. The values of x and y (BMN concentration) in the two systems ranged from 0.0 to 0.3 at regular intervals of 0.1. Raw materials used were oxide chemicals of 99.9% purity, except for PbO of >99.5%. In order to maintain the stoichiometries as close to the nominal values as possible, the moisture contents of the raw chemicals and of the

* Corresponding author. Tel.: +82 53 950 5636; fax: +82 53 950 5645.
E-mail address: nkkim@knu.ac.kr (N.-K. Kim).

0272-8842/$32.00 © 2006 Published by Elsevier Ltd and Techna Group S.r.l.
doi:10.1016/j.ceramint.2006.03.023

prepared precursors were measured and introduced into the batch calculations.

B-site precursor powders were separately prepared using oxide chemicals in appropriate proportions (Eqs. (1a) and (1b)). Powder batches were wet-milled (using ZrO_2 media) under alcohol for 24 h, dried overnight, and calcined at 1050–1200 and 1100–1200 °C in Systems I and II, respectively. PbO and Bi_2O_3 were then added to the synthesized powders also in stoichiometric ratios (Eqs. (2a) and (2b)) and the total batches were wet-milled, dried, and reacted at 800–850 °C for both systems. Phases formed after the calcination procedures were examined by X-ray diffraction (XRD, Cu Kα). After the addition of a polyvinyl alcohol binder (2 wt.% aqueous solution), the powders were uniaxially-formed into pellets, followed by further isostatic compaction. The preforms were fired for 2 h at 1000–1200 °C (System I) and 1000–1150 °C (System II), with intermediate binder burnout stage at 600 °C for 1 h. In order to suppress the evaporation of PbO and/or Bi_2O_3 at high temperatures, the firing procedures were carried out using a multiple-enclosure crucible setup [12], where the pellets were embedded in identical composition powders. Sintered pellets were ground/polished to attain parallel sides and gold-sputtered for electrical contacts. Dielectric constant and loss values were determined on cooling using an impedance analyzer under the conditions of $\sim 1 V_{rms}$/mm and 1–1000 kHz:

$$(0.8-x)(Mg_{1/3}Nb_{2/3})O_2 + x(Mg_{2/3}Nb_{1/3})O_{1.5} + 0.2TiO_2 \rightarrow (Mg_{(0.8+x)/3}Nb_{(1.6-x)/3}Ti_{0.2})O_{2-x/2} \quad (1a)$$

$$(0.7-y)(Mg_{1/3}Nb_{2/3})O_2 + y(Mg_{2/3}Nb_{1/3})O_{1.5} + 0.3TiO_2 \rightarrow (Mg_{(0.7+y)/3}Nb_{(1.4-y)/3}Ti_{0.3})O_{2-y/2} \quad (1b)$$

$$(1-x)PbO + (x/2)Bi_2O_3 + (Mg_{(0.8+x)/3}Nb_{(1.6-x)/3}Ti_{0.2})O_{2-x/2} \rightarrow (Pb_{1-x}Bi_x)(Mg_{(0.8+x)/3}Nb_{(1.6-x)/3}Ti_{0.2})O_3 \quad (2a)$$

$$(1-y)PbO + (y/2)Bi_2O_3 + (Mg_{(0.7+y)/3}Nb_{(1.4-y)/3}Ti_{0.3})O_{2-y/2} \rightarrow (Pb_{1-y}Bi_y)(Mg_{(0.7+y)/3}Nb_{(1.4-y)/3}Ti_{0.3})O_3 \quad (2b)$$

3. Results and discussion

Room-temperature XRD results in the two B-site precursor composition sets are compared in Figs. 1(a) and (b), where two major phases of $MgNb_2O_6$ and $[(Mg_{1/3}Nb_{2/3})_{1/2}Ti_{1/2}]O_2$ (columbite and rutile structures of ICDD Nos. 33–875 and 40–366, respectively) were identified. $MgNb_2O_6$ was the predominant phase throughout the compositions in Fig. 1(a), whereas fractions of $[(Mg_{1/3}Nb_{2/3})_{1/2}Ti_{1/2}]O_2$ were negligible to substantial. In Fig. 1(b), by contrast, intensities of the rutile were greater at $y = 0.0$–0.2, but those of the columbite were again higher at $y = 0.3$. Meanwhile $(Mg_{2/3}Nb_{1/3})O_{1.5}$ (i.e., $Mg_4Nb_2O_9$ of a corundum structure, ICDD No. 38–1459) was also detected at $x,y = 0.1$–0.3, though in small fractions.

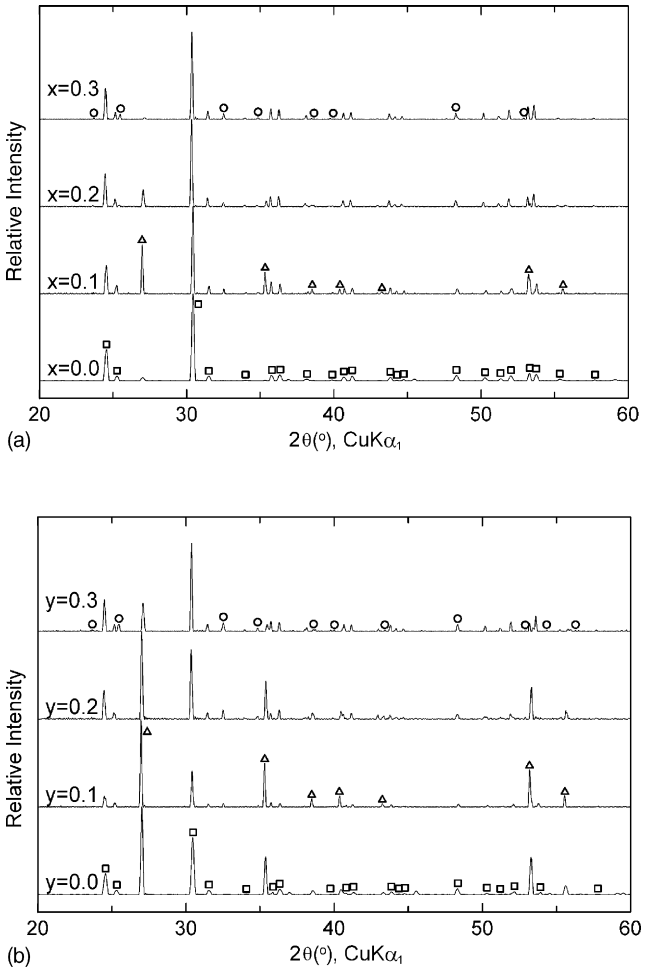

Fig. 1. X-ray traces in the B-site precursor compositions of: (a) $(0.8-x)(Mg_{1/3}Nb_{2/3})O_2$–$x(Mg_{2/3}Nb_{1/3})O_{1.5}$–$0.2TiO_2$ and (b) $(0.7-y)(Mg_{1/3}Nb_{2/3})O_2$–$y(Mg_{2/3}Nb_{1/3})O_{1.5}$–$0.3TiO_2$. (□) $MgNb_2O_6$, (△) $[(Mg_{1/3}Nb_{2/3})_{1/2}Ti_{1/2}]O_2$, and (○) $Mg_4Nb_2O_9$.

The phases developed in Systems I and II are contrasted in Figs. 2(a) and (b). In both systems, only typical patterns of a perovskite structure were observable without any trace of the parasitic pyrochlore, presence of which (even in small fractions) has been reported to be quite detrimental to dielectric properties [13–15]. The *h k l* indices are marked based upon the (pseudo)cubic symmetry of the perovskite structure. Extraneous peaks, associated with the formation of a perovskite superstructure, were not detected either, indicating absence of any long-range structural ordering (at least in the macroscopic scale) among the six-fold octahedral cation species of Mg, Nb, and Ti. Relative densities of the sintered ceramics were 92–93% of theoretical ($x,y = 0.0$) and 95–97% ($x,y = 0.1$–0.3), as determined using the perovskite lattice parameters.

Dielectric constant values of $x = 0.1$ (System I) and $y = 0.1$ (System II) are displayed in Fig. 3, where frequency dispersion of the dielectric maxima are well demonstrated. Numerical values of the maximum dielectric constant (K_{max}) and corresponding temperatures (T_{max}) are listed in Table 1, as a function of measurement frequency. Meanwhile, values of the dielectric loss ($\tan\delta$) were 10%, 11.5%, 13%, and 17%

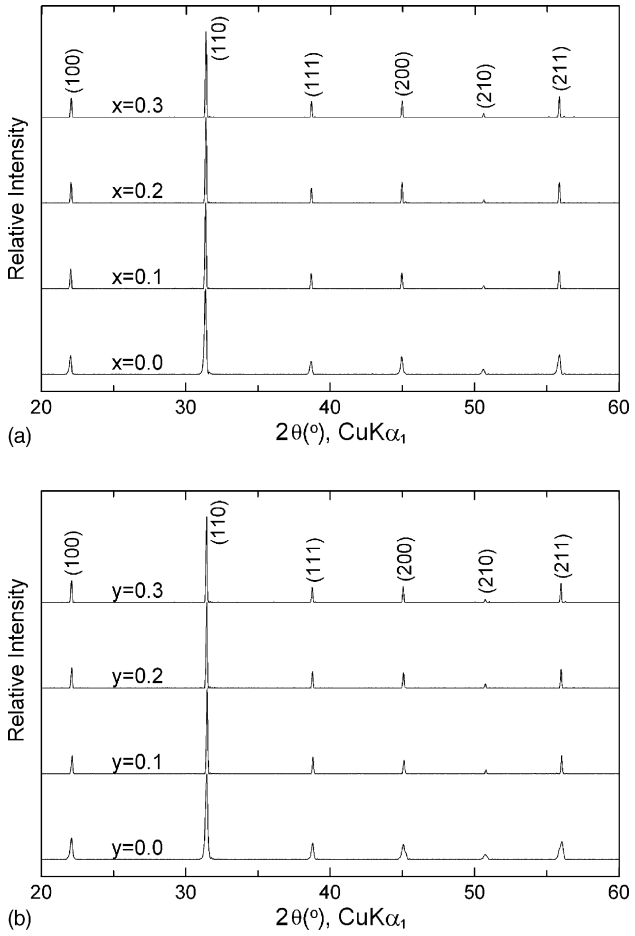

Fig. 2. Developed structures in the systems of: (a) $(0.8 - x)Pb(Mg_{1/3}Nb_{2/3})O_3$–$xBi(Mg_{2/3}Nb_{1/3})O_3$–$0.2PbTiO_3$ and (b) $(0.7 - y)Pb(Mg_{1/3}Nb_{2/3})O_3$–$yBi(Mg_{2/3}Nb_{1/3})O_3$–$0.3PbTiO_3$. (*h k l*) perovskite.

($x = 0.1$), and 7.5%, 9%, 11%, and 14% ($y = 0.1$) at temperatures of 30–40 °C lower than respective T_{max} values. Other compositions of the two systems also showed similar behavior of dielectric relaxation.

Temperature-dependent values of the dielectric constant in Systems I and II are shown in Fig. 4. In both systems, magnitudes of the maximum dielectric constant were highest at compositions without any BMN introduction: i.e., 29,300 and 25,000 at $x = 0.0$ and $y = 0.0$, respectively. The maximum values decreased tremendously to 6300 (System I) and 8050 (System II) at 10 mol% BMN concentration, followed by further decreases to 2350 ($x = 0.3$) and 3750 ($y = 0.3$). Moreover, the dielectric constant peaks gradually lost the symmetric modes (demonstrated at $x,y = 0.0$) with increasing BMN fraction and finally became almost linear in the paraelectric temperature ranges.

Table 1
Frequency-dependent K_{max} and T_{max} values of $x = 0.1$ and $y = 0.1$

Frequency	$x = 0.1$		$y = 0.1$	
	K_{max}	T_{max} (°C)	K_{max}	T_{max} (°C)
1 kHz	6300	41	8050	76
10 kHz	5950	45	7650	83
100 kHz	5600	52	7200	90
1 MHz	5150	64	6650	99

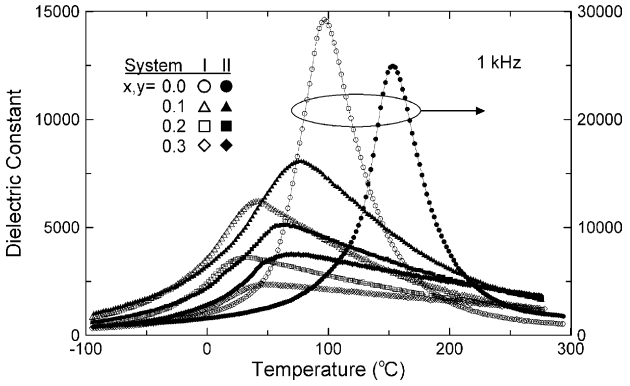

Fig. 4. Variations of the dielectric constant values in the two systems.

Variations of the maximum dielectric constant and corresponding temperature with compositional and frequency changes are plotted in Fig. 5. With increasing BMN concentration in both systems, the K_{max} values decreased rapidly in the ranges of $x,y = 0.0$–0.1 then somewhat slowly afterwards. Therefore, the sharply decreasing trend at the early stages of the Bi substitution at PMN-10PT [9] was not alleviated in the present systems, indicating harmful effect of Bi

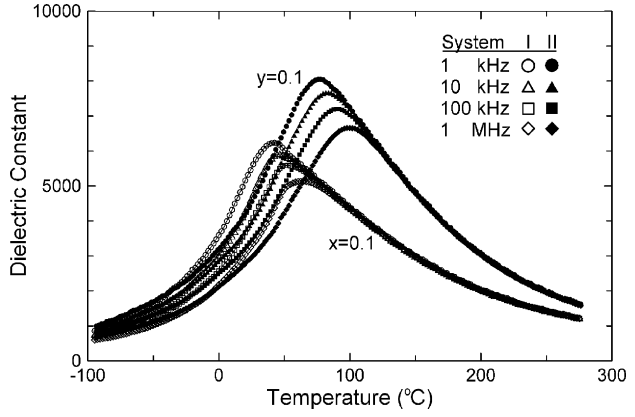

Fig. 3. Frequency-dependent dispersion in the dielectric constant values of $x,y = 0.1$.

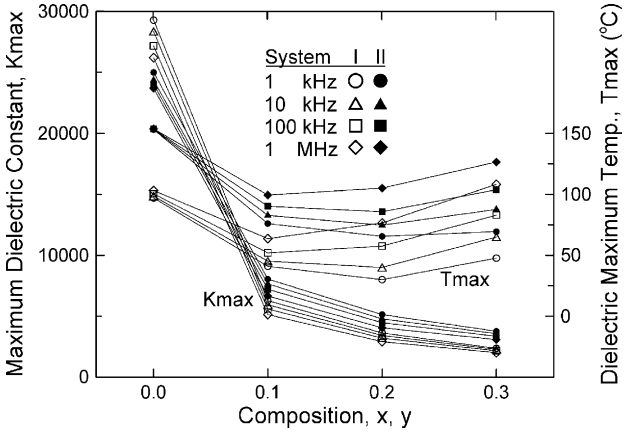

Fig. 5. Dependencies of the maximum dielectric constant and corresponding temperature upon compositional and frequency changes in Systems I and II.

on the long-range coupling of oxygen octahedra. Meanwhile, the values of K_{max} at $x,y = 0.0$ were greater in System I, but the magnitudes immediately became reversed and those of System II were greater at $0.1 \leq x,y$.

In contrast, variations of the dielectric maximum temperature with compositional change were not straightforward, similar to the trends in 10 mol% PT-substituted case [9]. Instead, the values were lowest at intermediate compositions of $x = 0.2$ (1 and 10 kHz) and $x = 0.1$ (100 and 1000 kHz), and $y = 0.2$ (1, 10, and 100 kHz) and $y = 0.1$ (1000 kHz). The overall results were somewhat contradictory to the reported increase in T_{max} with increasing fractions of Bi (replacing Pb) [16]. The values of ΔT_{max} ($T_{max,1\ MHz} - T_{max,1\ kHz}$) were 6, 21, 43, and 61 °C at $x = 0.0$–0.3, and 1, 23, 40, and 57 °C at $y = 0.0$–0.3. It is interesting to note that the ΔT_{max} values depended heavily upon the BMN concentration of x and y, but not as much on the PT fraction in the two systems. Additionally, differences between the dielectric maximum temperatures of Systems I and II ($T_{max,II} - T_{max,I}$) were rather insensitive to the frequency change: e.g., 56, 55, 53, and 51 °C in the four frequency decades at $x,y = 0.0$. However, the values became progressively smaller with increasing BMN fraction and finally were 22, 23, 21, and 18 °C at $x,y = 0.3$.

4. Summary

Phases of $MgNb_2O_6$ and $[(Mg_{1/3}Nb_{2/3})_{1/2}Ti_{1/2}]O_2$ (along with small fractions of $Mg_4Nb_2O_9$ at $x,y = 0.1$–0.3) were identified in both sets of the B-site precursor compositions. The former phase was predominant at $x = 0.0$–0.3 and $y = 0.3$, whereas intensities of the latter were greater at $y = 0.0$–0.2. Meanwhile, only typical patterns of a perovskite structure (without any diffraction peaks by superstructure formation) were developed in Systems I and II, after the addition of PbO and Bi_2O_3. Frequency-dependent dielectric dispersion behavior was observed throughout the investigated compositions in the two systems. However, degree of the relaxation became more pronounced with increasing values of x and y. Magnitudes of the maximum dielectric constant decreased rapidly then slowly from 29,300 to 2350 (System I) and from 25,000 to 3750 (System II) at 1 kHz with increasing BMN concentrations. By contrast, the dielectric maximum temperatures were lowest at intermediate compositions: e.g., $x,y = 0.2$ at 1 kHz.

Acknowledgement

This study was supported by the Korea Research Foundation under Grant No. KRF-2004-002-D00172.

References

[1] Y. Yamashita, PZN-based relaxors for MLCCs, Am. Ceram. Soc. Bull. 73 (8) (1994) 74–80.
[2] M.-C. Chae, S.-M. Lim, N.-K. Kim, Stabilization of perovskite phase and enhancement in dielectric properties by substitution of $Pb(Mg_{1/3}Nb_{2/3})O_3$ to $Pb(Zn_{1/3}Ta_{2/3})O_3$, Ferroelectrics 242 (1–4) (2000) 25–35.
[3] D.-H. Suh, D.-H. Lee, N.-K. Kim, Phase developments and dielectric/ferroelectric responses in the PMN-PT system, J. Eur. Ceram. Soc. 22 (2) (2002) 219–223.
[4] S.L. Swartz, T.R. Shrout, Fabrication of perovskite lead magnesium niobate, Mater. Res. Bull. 17 (10) (1982) 1245–1250.
[5] S.L. Swartz, T.R. Shrout, W.A. Schulze, L.E. Cross, Dielectric properties of lead magnesium niobate ceramics, J. Am. Ceram. Soc. 67 (5) (1984) 311–315.
[6] R.D. Shannon, Revised effective ionic radii and systematic studies of interatomic distances in halides and chalcogenides, Acta Crystallogr. A32 (5) (1976) 751–767.
[7] A.N. Salak, A.D. Shilin, M.V. Bushinski, N.M. Olekhnovich, N.P. Vyshatko, Structural regularities and dielectric phenomena in the compound series $PbB^{3+}_{1/2}Nb_{1/2}O_3$, Mater. Res. Bull. 35 (9) (2000) 1429–1438.
[8] Y.-S. Kim, N.-K. Kim, Dielectric characteristics of bismuth-modified lead magnesium niobate ceramics, Mater. Res. Bull. 39 (9) (2004) 1177–1183.
[9] Y.-S. Kim, N.-K. Kim, Dielectric characteristics of Bi- and Ti-substituted $Pb(Mg_{1/3}Nb_{2/3})O_3$, J. Am. Ceram. Soc. 88 (12) (2005) 3525–3527.
[10] B.-H. Lee, N.-K. Kim, J.-J. Kim, S.-H. Cho, Perovskite formation sequence by B-site precursor method and dielectric properties of PFW-PFN ceramics, Ferroelectrics 211 (1–4) (1998) 233–247.
[11] S. Ananta, N.W. Thomas, A Modified two-stage mixed oxide synthetic route to lead magnesium niobate and lead iron niobate, J. Eur. Ceram. Soc. 19 (2) (1999) 155–163.
[12] M.-C. Chae, N.-K. Kim, J.-J. Kim, S.-H. Cho, Preparation and dielectric properties of $Pb[(Mg_{1/3}Ta_{2/3}),(Zn_{1/3}Nb_{2/3})]O_3$ relaxor ceramics, Ferroelectrics 211 (1–4) (1998) 25–39.
[13] J. Chen, A. Gorton, H.M. Chan, M.P. Harmer, Effect of powder purity and second phases on the dielectric properties of lead magnesium niobate ceramics, J. Am. Ceram. Soc. 69 (12) (1986) C303–C305.
[14] T.R. Shrout, A. Halliyal, Preparation of lead-based ferroelectric relaxors for capacitors, Am. Ceram. Soc. Bull. 66 (4) (1987) 704–711.
[15] M.F. Yan, H.C. Ling, W.W. Rhodes, Preparation and properties of PbO–MgO–Nb_2O_5 ceramics near the $Pb(Mg_{1/3}Nb_{2/3})O_3$ composition, J. Mater. Res. 4 (4) (1989) 930–944.
[16] S.J. Butcher, N.W. Thomas, Ferroelectricity in the system $Pb_{1-x}Ba_x(Mg_{1/3}Nb_{2/3})O_3$, J. Phys. Chem. Solids 52 (4) (1991) 595–601.